

UCRL-JRNL-225431



LAWRENCE  
LIVERMORE  
NATIONAL  
LABORATORY

# Combined Climate and Carbon-Cycle Effects of Large-Scale Deforestation

G. Bala, K. Caldeira, M. Wickett, T. J. Phillips, D.  
B. Lobell, C. Delire, A. Mirin

October 20, 2006

Proceedings of the National Academy of Sciences

## **Disclaimer**

---

This document was prepared as an account of work sponsored by an agency of the United States Government. Neither the United States Government nor the University of California nor any of their employees, makes any warranty, express or implied, or assumes any legal liability or responsibility for the accuracy, completeness, or usefulness of any information, apparatus, product, or process disclosed, or represents that its use would not infringe privately owned rights. Reference herein to any specific commercial product, process, or service by trade name, trademark, manufacturer, or otherwise, does not necessarily constitute or imply its endorsement, recommendation, or favoring by the United States Government or the University of California. The views and opinions of authors expressed herein do not necessarily state or reflect those of the United States Government or the University of California, and shall not be used for advertising or product endorsement purposes.

**Classification:** Physical Sciences (major), Environmental Sciences  
(minor)

**Title: Combined Climate and Carbon-Cycle Effects of  
Large-Scale Deforestation**

G. Bala<sup>1</sup>, K. Caldeira<sup>2</sup>, M. Wickett<sup>1</sup>, T. J. Phillips<sup>1</sup>, D. B. Lobell<sup>1</sup>, C. Delire<sup>3</sup>, & A.  
Mirin<sup>1</sup>

<sup>1</sup>*Energy and Environment Directorate, Lawrence Livermore National Laboratory,  
Livermore, CA 94550, USA*

<sup>2</sup>*Department of Global Ecology, Carnegie Institution, Stanford, CA, USA*

<sup>3</sup>*Université Montpellier II, 34095 Montpellier cedex 5, France*

**Corresponding Author :**

G. Bala,  
L-103, Energy and Environment Directorate,  
Lawrence Livermore National Laboratory  
Livermore, CA 94550, USA  
Tel: 925 423 0771  
Fax: 925 422 6388  
Email: [bala1@llnl.gov](mailto:bala1@llnl.gov)

**Manuscript Information:**

Number of text pages: 14  
Number of Table pages: 1  
Number of Figure pages: 4

**Word and Character counts:**

Number of words in abstract: 187  
Number of character in the paper: 38, 872 with spaces

## Abstract

The prevention of deforestation and promotion of afforestation have often been cited as strategies to slow global warming. Deforestation releases CO<sub>2</sub> to the atmosphere, which exerts a warming influence on Earth's climate. However, biophysical effects of deforestation, which include changes in land surface albedo, evapotranspiration, and cloud cover also affect climate. Here we present results from several large-scale deforestation experiments performed with a three-dimensional coupled global carbon-cycle and climate model. These are the first such simulations performed using a fully three-dimensional model representing physical and biogeochemical interactions among land, atmosphere, and ocean. We find that global-scale deforestation has a net cooling influence on Earth's climate, since the warming carbon-cycle effects of deforestation are overwhelmed by the net cooling associated with changes in albedo and evapotranspiration. Latitude-specific deforestation experiments indicate that afforestation projects in the tropics would be clearly beneficial in mitigating global-scale warming, but would be counterproductive if implemented at high latitudes and would offer only marginal benefits in temperate regions. While these results question the efficacy of mid- and high-latitude afforestation projects for climate mitigation, forests remain environmentally valuable resources for many reasons unrelated to climate.

Deforestation affects the global climate both by releasing the carbon stored in the living plants and soils, and by altering the physical properties of the planetary surface. Deforestation exerts a warming influence by 1) adding CO<sub>2</sub> to the atmosphere, 2) eliminating the possible increased carbon storage in trees as a result of future CO<sub>2</sub>-fertilization and 3) decreasing evapotranspiration, particularly in the tropics(1-6). However, deforestation also exerts a cooling influence by 4) decreasing the surface albedo, particularly in seasonally snow-covered high-latitudes (7-10). We will refer to the first two climate effects that are mediated by changes in atmospheric carbon dioxide content as “carbon-cycle effects” and refer to the other two climate effects of forests as “biophysical effects”.

Since CO<sub>2</sub> is well mixed in the atmosphere, carbon-cycle effects are manifested globally, but biophysical effects are most strongly felt at regional scales. While the carbon-cycle effects have been taken into account in the promotion of afforestation as a climate change mitigation strategy, the biophysical effects of land-cover change have been largely ignored(11).The investigation of the combined carbon-cycle and climate effects of deforestation on the global climate is the subject of this paper.

The relative importance of carbon-cycle and albedo effects can be quantified in terms of radiative forcing(7), but the complexity of the climate response to changes in hydrological cycle challenges the application of such a metric(12) to changes in evapotranspiration . Evapotranspiration changes trigger atmospheric water vapor, cloud, and lapse-rate changes that produce local and global temperature changes. Previous studies have shown that deforestation in the tropics would decrease evapotranspiration rates and increase sensible heat fluxes, resulting in regionally decreased precipitation and increased surface temperature (1-3, 5, 13, 14).

Past studies have investigated the biophysical effects of deforestation in specific climatic zones(1-5, 8, 13, 15), of global deforestation(16-19), or of the combined biophysical and carbon-cycle effects of deforestation at different latitudes using simple models (7, 20-22). Here, we employ the Lawrence Livermore National Laboratory INCCA (Integrated Climate and Carbon) model(23, 24) to investigate transient carbon/climate interactions from year 2000 to 2150. Our study is the first to investigate the combined climate and carbon-cycle effects of deforestation in a fully interactive three-dimensional climate model that incorporates complex sub-models of vegetation dynamics, and terrestrial and oceanic components of the carbon-cycle(23-25).

### **Model Experiments**

In this study, we discuss six INCCA model simulations starting from the year 2000. In a “Standard” experiment without deforestation effects, CO<sub>2</sub> emissions follow historical levels for the period 1870-2000, SRES A2 levels (26) for the period 2000-2100, and a logistic function(23) for 2100-2150. This Standard simulation, which has been extensively discussed in our previous INCCA modeling studies(23-25), produces a global-mean warming in year 2100 that is 3.2 K greater than that of a “Control” simulation in which there is no CO<sub>2</sub> emissions and other greenhouse gases are fixed at pre-industrial levels. Four other experiments with different configurations of large-scale deforestation also are simulated. A “Global” experiment which brackets the climatic effects of global-scale deforestation, is identical to the Standard experiment except that plant functional types representing trees are not allowed to exist after year 2000, and thus only shrub and grass plant functional types remain. The biomass in tree leaves and fine roots is immediately transferred to the litter pool in year 2000, and the stem biomass becomes litter on a time scale of about 10 to 50 years depending on the tree plant functional type. In this simulation, the total carbon released to the atmosphere from tree functional types in the 21<sup>st</sup> century is 818 PgC.

To isolate the net effects of large-scale deforestation implemented in tropical, temperate and Northern high-latitudes, we consider three additional simulations where deforestation is restricted to the latitude bands 20°S-20°N (“Tropical”), 20°-50° in both the Northern and Southern Hemispheres (“Temperate”) and 50°-90° in the Northern Hemisphere (“Boreal”), respectively. The corresponding amounts of carbon released from trees in these latitude-band deforestation cases in the 21<sup>st</sup> century are 422, 316 and 80 PgC. Note that the sum of carbon lost from tree plant functional types in these three latitude-band simulations is equivalent to the tree carbon lost in the Global simulation.

## **Results**

Atmospheric CO<sub>2</sub> content is greater in the Global deforestation experiment both because of the release of carbon stored in trees in the early 21<sup>st</sup> century and the loss of CO<sub>2</sub>-fertilization of forested ecosystems seen in the Standard simulation (Fig. 1). Despite higher atmospheric CO<sub>2</sub> concentrations, the global- and annual-mean temperature in the Global experiment is cooler by about 0.3 K than the Standard case. Thus, on a global-mean basis, the warming carbon-cycle effects of deforestation are overwhelmed by the cooling biophysical effects.

The global-mean temperature differences relative to the Standard case in year 2100 in the Tropical, Temperate, and Boreal experiments, are +0.7 K, -0.04 K, and -0.8 K, respectively (Fig. 1), implying that the combined carbon-cycle and biophysical effects from tropical, temperate, and boreal deforestation are, respectively, net cooling, near-zero temperature change, and net warming. These latitude-band experiments thus suggest that projects in the tropics promoting afforestation are likely to slow down global warming, but such projects would offer only little to no climate benefits when implemented in temperate regions, and would be counterproductive, from a climate-perspective at higher latitudes.

The linear sum of the area-weighted global-mean temperature change over all the latitude-band experiments is -0.1 K in the year 2100. This value is close to the corresponding -0.3 K temperature change of the Global deforestation simulation, suggesting a near-linear behavior of the large-scale climate system despite the many non-linear processes represented by the INCCA model. The linear sum is slightly larger because, in the latitude-band experiments, our dynamic vegetation model allows the forests to expand in the regions which are not deforested(23, 27), and forests have lower albedo and absorb more solar radiation than grasses. The presence of trees in the latitude-band deforestation experiments and the consequent higher CO<sub>2</sub>-fertilization causes the linear sum of CO<sub>2</sub> changes from the Tropical, Temperate, and Boreal experiments to be lower than that of Global by 67 ppmv in year 2100.

Since the linear sum of the temperature response from latitude-band experiments is approximately equal to that of the Global experiment (Fig. 1), we focus our analysis on our global-scale deforestation simulation for brevity. The removal of forests in Global results in an atmospheric CO<sub>2</sub> concentration at year 2100 that is 381 ppmv greater than in the Standard simulation (1113 versus 732 ppmv; Fig. 1). In the Standard A2 scenario, 1790 PgC carbon is emitted to the atmosphere over the 21<sup>st</sup> century (Fig. 2). By year 2100, the terrestrial biosphere in the Global deforestation experiment has 972 Pg less carbon than in the Standard case. About 82 % (799 PgC) of this carbon resides in the atmosphere, with the oceans taking up the remaining 18 % (173 PgC). The ocean uptake increases in Global (444 vs 271 PgC in Standard A2) because the higher atmospheric CO<sub>2</sub> concentration drives an increased flux of carbon into the oceans.

The spatial distribution of climate and carbon-cycle changes in the Global simulation for the decade centered on year 2100 is shown in Figure 3A. Similar to the global-mean statistics, the linear sum (Fig. 3B) of the *spatial pattern* of temperature response from the latitude-specific Boreal, Temperate, and Tropical deforestation



experiments (Figs. 3C, 3D, and 3E) is also approximately equal to that of the Global experiment (Fig. 3A). This once again highlights the apparent linear response of the large-scale climate system despite the presence of many non-linear processes.

The spatial pattern of temperature differences suggests that the strongest cooling in Global deforestation is associated with the removal of boreal forests in the Northern Hemisphere high-latitudes (Fig. 3A, Table 1). The replacement of these forests by grasses and shrubs increases the surface albedo (brightens the surface) by as much as 0.25 (Fig. 4A). This results in decreased absorption of surface solar radiation and cooling that exceeds 6 K in some locations, despite higher CO<sub>2</sub> concentrations and high-latitude amplification of CO<sub>2</sub>-induced warming (28). The albedo effect therefore dominates the climate response in the Northern Hemisphere mid- and high-latitudes.

In the tropics, however, increases in surface albedo changes (Fig. 4A; Table 1) do not produce as much cooling, largely due to the changes in clouds. The removal of forests also decreases evapotranspiration (Fig. 4B), resulting in a decrease of clouds (Fig. 4C). Thus, the replacement of tropical forests with grass and shrub lands brightens the surface, but the decrease of clouds tends to darken the planet. These effects nearly cancel each other so that the planetary albedo at the top of the atmosphere (Fig. 4D) changes little over tropical regions. This suggests that cloud feedbacks initiated by evapotranspiration changes play a major role in determining the overall climatic impact of deforestation in the tropics.

Despite higher atmosphere CO<sub>2</sub> concentrations, the average annual-mean surface temperature over land in the Global deforestation experiment is cooler by 2.1 K, 1.6 K, and 0.4 K than that of the Standard experiment in the Northern Hemisphere high-latitudes (50°N to 90°N), mid-latitudes (20°N to 50°N), and tropics (20°S to 20°N), respectively (Table 1). In contrast, the Southern Hemisphere mid-latitude (50°S to 20°S)

land surface warms by 0.1 K. In the Northern Hemisphere mid- and high-latitudes, surface albedo effects dominate, resulting in decreased net surface solar absorption and cooling. In the tropics and Southern Hemisphere mid-latitudes, the surface albedo decrease is comparable to that in the Northern Hemisphere mid-latitudes (Table 1), but the decreases in evapotranspiration and cloudiness lead to increases in the surface incident and absorbed solar radiation which tend to warm the surface. However, the net biophysical effect is still cooling, and it is larger than the warming carbon-cycle effects in the tropics, while being only slightly smaller in the Southern Hemisphere mid-latitudes (Figure. 3A).

## Discussion

The approximate global-mean warming from carbon-cycle effects and cooling from biophysical effects can be estimated from our model's known climate sensitivity of 2.1 K and radiative forcing of  $3.5 \text{ Wm}^{-2}$  per doubling of  $\text{CO}_2$  (28). The extra radiative forcing in the Global experiment due to the excess 381 ppmv of  $\text{CO}_2$  at year 2100 would produce an equilibrium carbon-cycle warming of about 1.3 K. If we further assume that the transient temperature difference of 0.3 K between the Global and Standard experiments (Fig. 1A) remains the same at equilibrium, the cooling from net biophysical effects is about 1.6 K.

The INCCA terrestrial biosphere component model IBIS2 has higher carbon uptake with increased atmospheric  $\text{CO}_2$  than similar models(29). This model anomaly would tend to accentuate the simulated difference between the atmospheric  $\text{CO}_2$  in our deforestation simulations relative to our Standard simulation, thereby overestimating the warming carbon-cycle effects of global-scale deforestation relative to its biophysical cooling effects. With a less responsive biosphere model, we would expect to see even more cooling as a result of deforestation. The magnitude of the model-predicted net

cooling from large-scale deforestation thus may be greater than what would actually be seen. Further study is needed to confirm and better quantify our results.

Many of our conclusions are consistent with inferences drawn from previous studies that focused solely on radiative forcing(7) or employed simpler climate models(20-22): the climate effects of CO<sub>2</sub> storage in forests are offset by albedo changes at high latitudes, so that from a climate change mitigation perspective, projects promoting large-scale afforestation projects are likely to be counterproductive in these regions.

We find that tropical deforestation contributes to global warming both from carbon-cycle and biophysical effects (Fig. 3E), supporting conclusions drawn in earlier studies(20). The tropical cooling seen in the Global experiment (Table 1) therefore implies the presence of remote effects of deforestation implemented elsewhere (30-33). Nonetheless, this net tropical temperature change is small, and so its sign may be sensitive to the representation of physical processes such as cloud dynamics and surface hydrology in the model(34).

The results presented here highlight the need to employ climate-carbon models in order to comprehensively evaluate the carbon-cycle and biophysical effects of forests on climate. For example, although the importance of time-horizon in defining tradeoffs between carbon and biophysical effects is evident (e.g. increasing ocean uptake in Figure 2), this aspect of the problem has been largely overlooked in previous assessments. Another new policy-relevant implication is that large-scale afforestation implemented in temperate latitudes may be largely ineffectual in mitigating global warming. We note, however, that results for specific forest species in particular locations could vary from the global-scale results presented here. Furthermore, because carbon-cycle effects are manifested globally while biophysical effects are most strongly

felt locally, a particular afforestation project could produce regional warming while cooling the remainder of the planet.

Finally, we must bear in mind that preservation of ecosystems is a primary goal of preventing global warming, and the destruction of ecosystems to prevent global warming would be a counterproductive and perverse strategy. Therefore, the cooling that could potentially arise from deforestation outside the tropics should not necessarily be viewed as a strategy for mitigating climate change since, apart from their potential climatic role, forests are crucial in preserving the biodiversity of natural ecosystems. In planning responses to global challenges, it is important to pursue broad goals and to avoid narrow criteria which may lead to environmentally harmful consequences.

### **Acknowledgements**

This work was performed under the auspices of the U.S. Department of Energy by the University of California Lawrence Livermore National Laboratory under contract No. W-7405-Eng-48.

## References and Notes

1. Sud, Y. C., Yang, R. & Walker, G. K. (1996) *Journal of Geophysical Research-Atmospheres* **101**, 7095-7109.
2. Lean, J. & Rowntree, P. R. (1997) *Journal of Climate* **10**, 1216-1235.
3. Hahmann, A. N. & Dickinson, R. E. (1997) *Journal of Climate* **10**, 1944-1964.
4. Snyder, P. K., Foley, J. A., Hitchman, M. H. & Delire, C. (2004) *Journal of Geophysical Research-Atmospheres* **109**, D21102, doi:10.1029/2003JD004462.
5. Hendersonellers, A., Dickinson, R. E., Durbidge, T. B., Kennedy, P. J., Mcguffie, K. & Pitman, A. J. (1993) *Journal of Geophysical Research-Atmospheres* **98**, 7289-7315.
6. Dickinson, R. E. & Kennedy, P. (1992) *Geophysical Research Letters* **19**, 1947-1950.
7. Betts, R. A. (2000) *Nature* **408**, 187-190.
8. Bonan, G. B., Pollard, D. & Thompson, S. L. (1992) *Nature* **359**, 716-718.
9. Govindasamy, B., Duffy, P. B. & Caldeira, K. (2001) *Geophysical Research Letters* **28**, 291-294.
10. Brovkin, V., Ganopolski, A., Claussen, M., Kubatzki, C. & Petoukhov, V. (1999) *Global Ecology and Biogeography* **8**, 509-517.
11. Watson R.T., N. I. R., Bolin B., Ravindranath N.H., Verardo D.J., Dokken D.J. (2000) (Cambridge University Press, Cambridge, U.K.).
12. Boucher, O., Myhre, G. & Myhre, A. (2004) *Climate Dynamics* **22**, 597-603.
13. Costa, M. H. & Foley, J. A. (2000) *Journal of Climate* **13**, 18-34.
14. Werth, D. & Avissar, R. (2004) *Journal of Hydrometeorology* **5**, 100-109.
15. Foley, J. A., Kutzbach, J. E., Coe, M. T. & Levis, S. (1994) *Nature* **371**, 52-54.
16. Fraedrich, K., Kleidon, A. & Lunkeit, F. (1999) *Journal of Climate* **12**, 3156-3163.
17. Gibbard, S., Caldeira, K., Bala, G., Phillips, T. J. & Wickett, M. (2005) *Geophysical Research Letters* **32**, L23705, doi:10.1029/2005GL024550.
18. Kleidon, A., Fraedrich, K. & Heimann, M. (2000) *Climatic Change* **44**, 471-493.
19. Renssen, H., Goosse, H. & Fichefet, T. (2003) *Geophysical Research Letters* **30**, 1061, doi:10.1029/2002GL016155.
20. Claussen, M., Brovkin, V. & Ganopolski, A. (2001) *Geophysical Research Letters* **28**, 1011-1014.
21. Sitch, S., Brovkin, V., von Bloh, W., van Vuuren, D., Assessment, B. E. N. E. & Ganopolski, A. (2005) *Global Biogeochemical Cycles* **19**, GB2013, doi:10.1029/2004GB002311.
22. Schaeffer, M., Eickhout, B., Hoogwijk, M., Strengers, B., van Vuuren, D., Leemans, R. & Opsteegh, T. (2006) *Global Biogeochemical Cycles* **20**, GB2020, doi:10.1029/2005GB002581.
23. Bala, G., Caldeira, K., Mirin, A., Wickett, M. & Delire, C. (2005) *Journal of Climate* **18**, 4531-4544.
24. Thompson, S. L., Govindasamy, B., Mirin, A., Caldeira, K., Delire, C., Milovich, J., Wickett, M. & Erickson, D. (2004) *Geophysical Research Letters* **31**, L23211, doi:10.1029/2004GL021239.
25. Govindasamy, B., Thompson, S., Mirin, A., Wickett, M., Caldeira, K. & Delire, C. (2005) *Tellus Series B-Chemical and Physical Meteorology* **57**, 153-163.
26. Nakicenovic, N., Alcamo, J., Davis, G., Vries, B. d., Fenhann, J., Gaffin, S., Gregory, K., Grübler, A., Jung, T. Y., Kram, T., Rovere, E. L. L., Michaelis, L.,

- Mori, S., Morita, T., Pepper, W., Pitcher, H., Price, L. & Riahi, K. (2000) (Cambridge University Press, Cambridge, U.K.), pp. 599.
27. Bala, G., Caldeira, K., Mirin, A., Wickett, M., Delire, C. & Phillips, T. J. (2006) *Tellus Series B-Chemical and Physical Meteorology* **58**, 620-627.
  28. Intergovernmental Panel on Climate Change (IPCC) (2001) *Climate Change The Scientific Basis. Contribution of the Working Group I to the Third Assessment of the IPCC*, eds. Houghton, J. T., Ding, Y., Griggs, D. J., Noguer, M., van der Linden P. J., D. Xiaosu (Cambridge University Press Cambridge, U. K.).
  29. Cramer, W., Bondeau, A., Woodward, F. I., Prentice, I. C., Betts, R. A., Brovkin, V., Cox, P. M., Fisher, V., Foley, J. A., Friend, A. D., Kucharik, C., Lomas, M. R., Ramankutty, N., Sitch, S., Smith, B., White, A. & Young-Molling, C. (2001) *Global Change Biology* **7**, 357-373.
  30. Chase, T. N., Pielke, R. A., Kittel, T. G. F., Nemani, R. R. & Running, S. W. (2000) *Climate Dynamics* **16**, 93-105.
  31. Pielke, R. A., Marland, G., Betts, R. A., Chase, T. N., Eastman, J. L., Niles, J. O., Niyogi, D. D. S. & Running, S. W. (2002) *Philosophical Transactions of the Royal Society of London Series a-Mathematical Physical and Engineering Sciences* **360**, 1705-1719.
  32. Gedney, N. & Valdes, P. J. (2000) *Geophysical Research Letters* **27**, 3053-3056.
  33. Werth, D. & Avissar, R. (2002) *Journal of Geophysical Research-Atmospheres* **107**, 8087, doi:10.1029/2001JD000717.
  34. Osborne, T. M., Lawrence, D. M., Slingo, J. M., Challinor, A. J. & Wheeler, T. R. (2004) *Climate Dynamics* **23**, 45-61.

## Figure Legends

**Figure 1** Simulated temporal evolution of a) atmospheric CO<sub>2</sub> and b) 10-year running of surface temperature change for the period 2000-2150 in the Standard and deforestation experiments. Warming effects of increased atmospheric CO<sub>2</sub> are more than offset by the cooling biophysical effects of global deforestation in the Global simulation, producing a cooling relative to the Standard experiment of about 0.3 K around year 2100. The combined carbon-cycle and biophysical effects from Tropical, Temperate, and Boreal deforestation are net cooling, near-zero temperature change, and net warming, respectively. The sum of the temperature changes in the latitude-band experiments is approximately equal to the temperature change in the Global simulation, suggesting near-linearity.

**Figure 2** Simulated cumulative emissions and carbon stock changes in atmosphere, ocean, and land for the period 2000-2150 in A) Standard and B) Global experiments. In Standard, strong CO<sub>2</sub>-fertilization results in vigorous uptake and storage of carbon by land ecosystems. In the Global case, land ecosystem carbon is lost to the atmosphere as a result of global deforestation. Most of this carbon is ultimately reabsorbed by grasses and shrubs growing in a warmer CO<sub>2</sub>-fertilized climate at year 2100. Of the land ecosystem carbon in the Standard simulation that is not present in the land biosphere in the Global simulation at year 2100, 82 % resides in the atmosphere, and the remaining 18 % in the oceans.

**Figure 3** Simulated spatial surface temperature differences relative to the Standard experiment in the decade centered on year 2100 for A) Global and B) the linear sum of C) Boreal, D) Temperate, and E) Tropical deforestation experiments. Cooling biophysical effects of deforestation overwhelm warming

carbon-cycle effects over most of the land surface (including tropical regions), but are most pronounced in the Northern high latitudes. Comparison of A) and B) shows the near-linear behavior of the model climate system. Cooling biophysical effects of deforestation dominate the climate response in the Boreal deforestation case C). In the Temperate deforestation case D), there are strong local cooling responses though the global-mean response is near-zero. The carbon-cycle effects of warming overwhelm the biophysical effects in the Tropical deforestation case E) with slight local cooling responses from the biophysical effects.

**Figure 4** Simulated spatial pattern differences (Global minus Standard) in the decade centered on year 2100 for A) surface albedo (fraction), B) evapotranspiration (cm/day), C) cloudiness (fraction), and D) planetary albedo (fraction) differences. Albedo effects dominate the Northern Hemisphere mid- and high-latitude climate change and produce a strong cooling in Global relative to Standard. In the tropics and Southern Hemisphere land areas, the warming due to higher atmospheric CO<sub>2</sub> is largely offset by cooling biophysical effects, producing little net temperature change. In the tropics, removal of forests increases surface albedo (Fig. 4A) and decreases evapotranspiration (Fig. 4B). The reduction in evapotranspiration decreases cloudiness (Fig. 4C), which reduces albedo as seen from the top of the atmosphere (Fig. 4D), largely offsetting the effects of the increased surface albedo.



## Tables

**Table 1:** Climate variable differences between Global and Standard experiments for the decade centered on year 2100. Evapotranspiration percentage differences are relative to Standard mean climate for this period. Cloudiness and albedo changes are absolute changes.

|  | Global | Global Land | SH <sup>a</sup> mid-lat Land (50° S to 20° S) | Tropical Land(20° S to 20° N) | NH <sup>b</sup> mid-lat. Land (20° S to 50°N) | NH high-lat. Land (50°S to 90°N) |
|--|--------|-------------|---|-------------------------------|---|----------------------------------|
| Surface Temperature (K)                              | -0.3   | -1.0        | 0.1   | -0.4                          | -1.6  | -2.1                             |
| Evapo-transpiration (%)                              | -2.6   | -7.8        | -16.7   | -5.8                          | -5.8  | -14.6                            |
| Surface albedo(%)                                    | 1.9    | 5.2         | 5.0   | 4.1                           | 4.7   | 10.7                             |
| TOA <sup>c</sup> albedo (%)                          | 0.6    | 1.6         | 0.5   | -0.3                          | 1.7   | 5.5                              |
| Total cloudiness (%)                                 | -0.7   | -1.7        | -4.7  | -4.6                          | -1.2  | 2.5                              |
| Surface SW <sup>d</sup> absorbed (Wm <sup>-2</sup> ) | -1.4   | -4.3        | -1.7  | 1.2                           | -5.2  | -13.8                            |
| Surface downward SW (Wm <sup>-2</sup> )              | 2.2    | 5.1         | 11.3  | 12.9                          | 3.0   | -3.2                             |

<sup>a</sup> Southern Hemisphere, <sup>b</sup> Northern Hemisphere, <sup>c</sup> Top of Atmosphere, <sup>d</sup> Shortwave

Figure 1

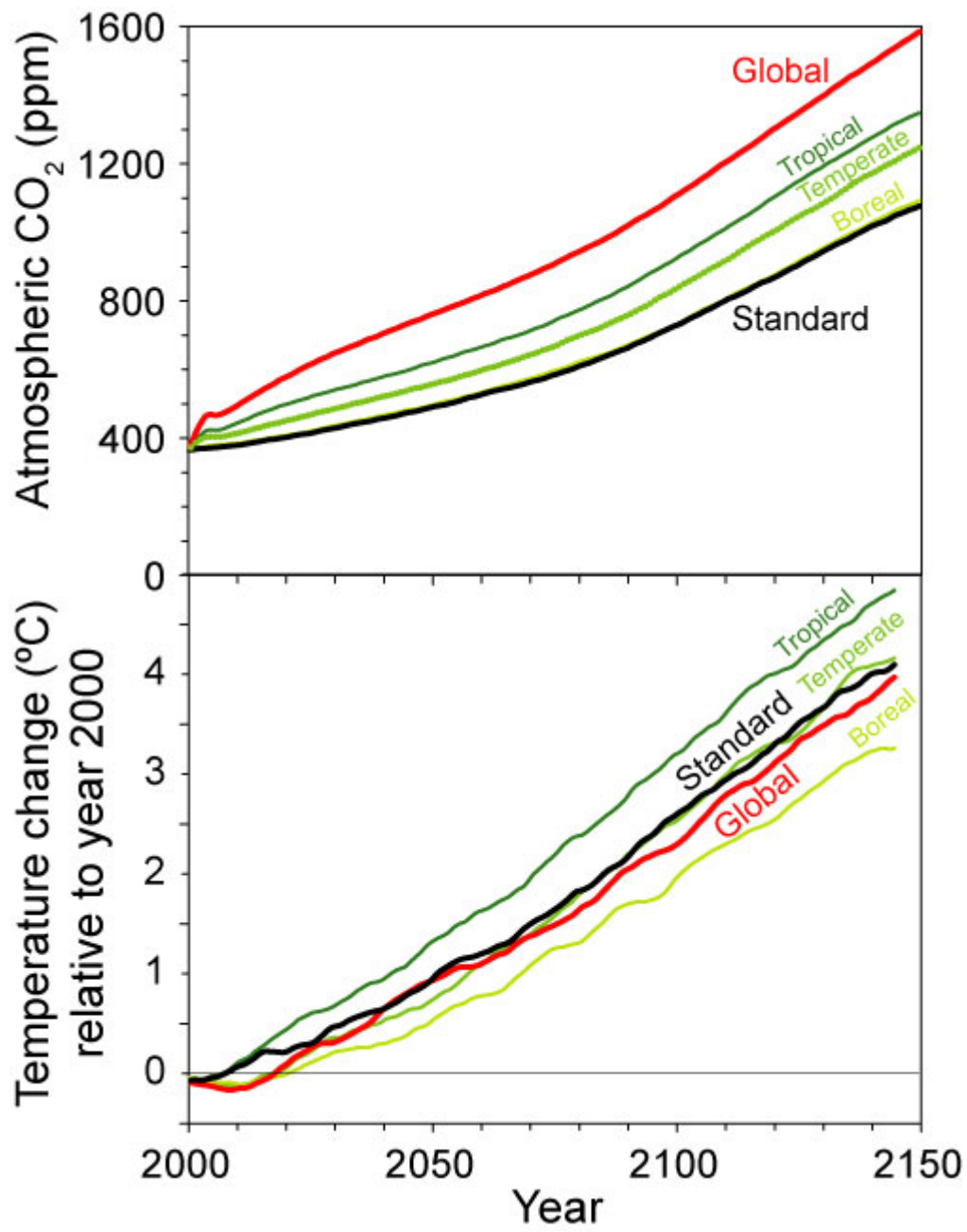


Figure 2

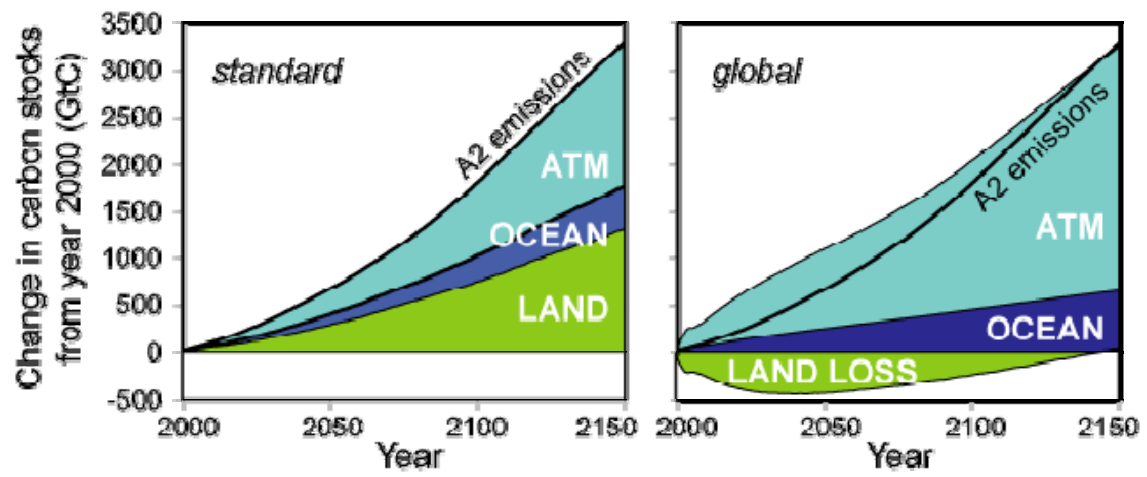


Figure 3

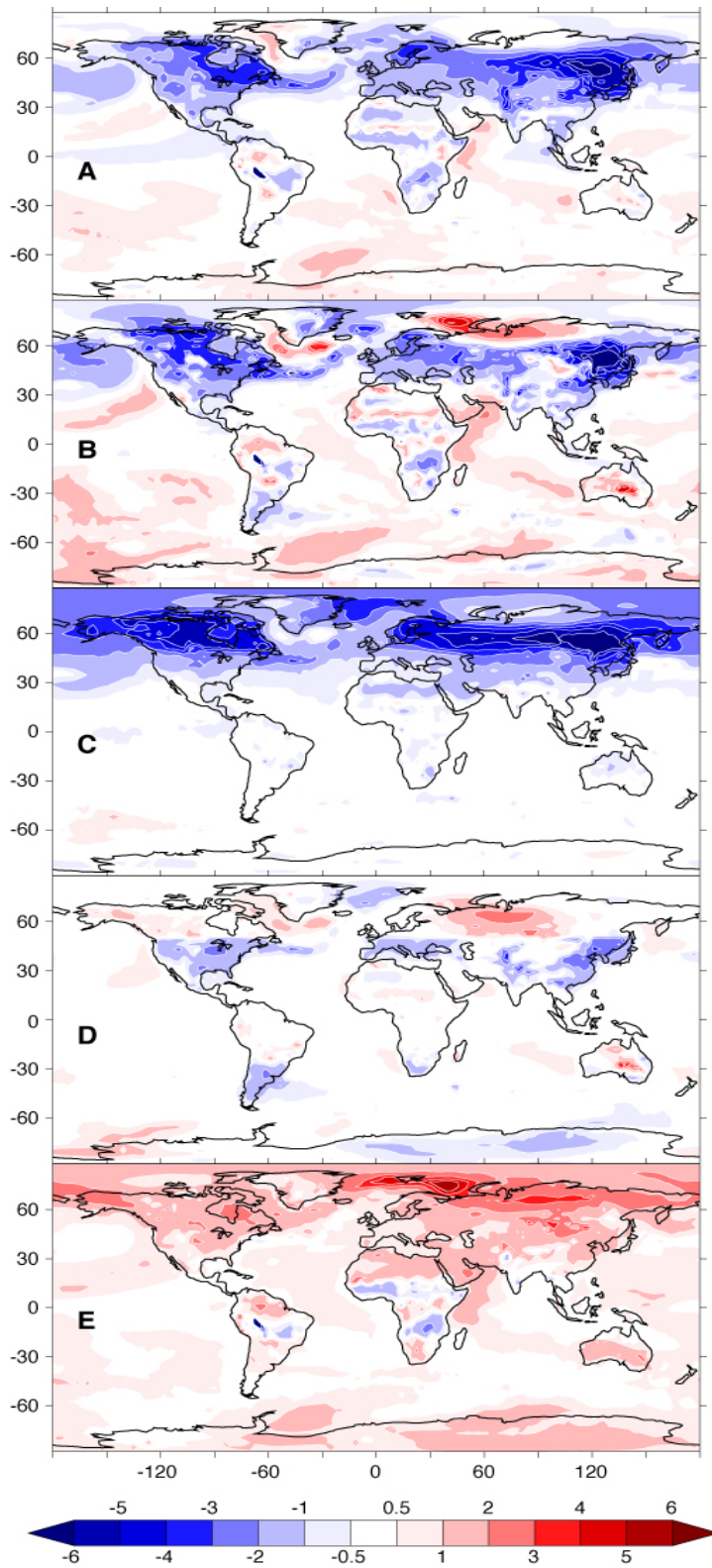


Figure 4

